

-Amplification of the Aerosol Direct Effect in Declining Global Emissions. -Strong Regional Variability in the Direct Effect of Anthropogenic Aerosols

Antoine Hermant¹, Linnea Huusko¹, Thorsten Mauritsen¹

¹Department of Meteorology, Stockholm University, Stockholm, Sweden

Key Points:

- Despite declining aerosol emissions, the modelled direct effect of anthropogenic aerosols has continued to increase.
- Insights from the shift in aerosol pattern throughout the 1970–2014 period has implication in the continued increase in direct effect.
- Regional variations in aerosol emission efficiency are associated with cloudiness, aerosol removal processes and surface albedo.

Corresponding author: Antoine Hermant, antoine.hermant74@gmail.com

Abstract

Anthropogenic aerosol particles partially mask global warming driven by greenhouse gases, both by directly reflecting sunlight back into space and indirectly by increasing cloud reflectivity, which also results in sunlight reflection. In recent decades, however, the emissions of anthropogenic aerosols have declined globally, and at the same time shifted from the North American and European regions to foremost Southeast Asia. Using global climate model simulations we find that the direct effect of aerosols has instead continued to increase, despite declining emissions, whereas the indirect effect has weakened in approximate proportion with the emissions. The enhanced efficiency of aerosol emissions to the induced negative forcing is associated with less cloudiness, longer atmospheric residence time, and emissions over darker surfaces in the Southeast Asian region.

Plain Language Summary

Aerosols, which are tiny particles in the atmosphere from natural sources and human activities, have a cooling effect on climate, partially masking global warming caused by greenhouse gases. They achieve this through both direct and indirect mechanisms. Directly, aerosols cool the climate by reflecting incoming sunlight, while indirectly, they alter cloud properties, increasing cloud reflectivity, further cooling the climate. In this study, we investigate the historical evolution of these effects using a global climate model. We discovered that despite their global decline, the direct effect of human-made aerosols on the climate has instead increased, while the indirect effect has decreased. We associate the increase in direct effect with the shift in aerosol spatial distribution that accompanied the decline. Our findings underscore the critical role of aerosol emission regions in climate impact, particularly evident for the indirect effect, which prevails in originally pristine areas. However, this regional dependence also applies to the direct effect, influenced by factors such as cloud cover, surface reflectivity (albedo), and the processes involved in aerosol removal from the atmosphere.

1 Introduction

Global climate models participating in the Coupled Model Intercomparison Project phase 6 (CMIP6) have indicated a higher climate sensitivity comparing to previous models (Flynn & Mauritsen, 2020). However, a majority of these models simulate a reduced historical warming, with global temperatures consistently cooler than actual observations from 1940 to 2000. Flynn et al. (2023) has demonstrated that strong aerosol cooling alone cannot account for this lack of warming in the mid-20th century.

CMIP6 models exhibit a wide range of anthropogenic aerosol forcing, which complicates efforts to constrain the total anthropogenic radiative forcing, especially due to intricate interactions with clouds (Bellouin et al., 2020). In the desire of an uniform and easily controlled representation of anthropogenic aerosol impacts within the CMIP6 framework (Eyring et al., 2016; Pincus et al., 2016), Stevens et al. (2017) introduced the MACv2-SP parametrisation. Using this latter, Huusko et al. (2022) investigated the relative contributions of direct and indirect aerosol effects on the climate response. Their work revealed that the indirect effect induces a stronger response due to cooling in remote regions. This highlights the importance of aerosol distribution in shaping the resulting forcing and cooling effect. Nonetheless, the relative contributions of these two effects throughout history remain uncertain, as aerosol spatial distribution has changed with evolving emission patterns (Stevens, 2015). Prior attempts to study the impact of aerosol distribution changes on effective radiative forcing, such as Fiedler et al. (2017) that found no significant difference between the aerosol patterns of the 1970s and 2000s.

In this study, we propose employing the Partial Radiative Perturbation method (Wetherald & Manabe, 1988; Colman & McAvaney, 1997; Klocke et al., 2013) for calculating aerosol

radiative forcing. We use this method alongside the simplified representation of anthropogenic aerosols from MACv2-SP in MPI-ESM1.2-CR, enabling the separation of direct and indirect effects. By using this approach, we can investigate the historical trends of both aerosol effects and gain insights into the mechanisms underlying the influence of aerosol distribution on the resulting radiative forcing.

2 Method

We study the historical evolution of the aerosol forcing using the Max Planck Institute for Meteorology Earth System Model version 1.2. MPI-ESM1.2, a state-of-the-art climate model (Mauritsen et al., 2019) that participated in the Coupled Model Intercomparison Project Phase 6 (CMIP6), successfully reproduces the observed warming from pre-industrial levels (Mauritsen & Roeckner, 2020). The radiative transfer scheme of MPI-ESM1.2 uses the Simple Plumes implementation of the second version of the Max Planck Institute Aerosol Climatology (MACv2-SP) to represent the aerosol impact on the radiation. MACv2-SP provides a parametrization of optical properties of anthropogenic aerosols and the resulting Twomey effect, accounting for aerosol-cloud interaction (Stevens et al., 2017). It has been designed with the desire of an uniform and easily controlled representation of anthropogenic aerosol perturbations for the CMIP6 framework (Eyring et al., 2016; Pincus et al., 2016). To achieve this, Stevens et al. (2017) constructed nine spatial plumes that are associated with emissions from major anthropogenic source regions. They used aerosol optical properties estimates from ground-based measurements provided by the Max Planck Institute Aerosol Climatology, MAC (Kinne et al., 2013), for the present-day (2005) distribution of mid-visible anthropogenic aerosol optical depth (AOD). To represent changes from pre-industrial (1850) to 2016, they scaled the present-day distribution using historical emission data obtained from the Community Emissions Data System (CEDS). Two types of plumes are considered: industrial for Europe, North America, Australia, East and South Asia and biomass burning for South America, Maritime Continental, North and South Central Africa. These two types differ in seasonal cycle amplitude, single-scattering albedo and strength in Twomey effect. To model the Twomey effect, Stevens et al. (2017) used satellite observations to derive the relationship between the cloud droplet number density and the fine-mode AOD. Through this representation, anthropogenic aerosols cause a greater increase in cloud optical thickness when the atmospheric environment is initially pristine in terms of aerosols. For the complete description of MACv2-SP, refer to Stevens et al. (2017).

Meraner et al. (2013) and Block and Mauritsen (2013) implemented in MPI-ESM the two-sided Partial Radiative Perturbation method (PRP) described in Klocke et al. (2013). The PRP method has first been described by Wetherald and Manabe (1988) and Colman and McAvaney (1997). This method was designed to evaluate the respective contributions of individual climate feedbacks (water vapor, temperature, clouds and surface albedo) on the radiative imbalance. In our study, we integrated the anthropogenic aerosol perturbation provided from MACv2-SP into the PRP module of MPI-ESM1.2. This integration enables us to estimate the instantaneous radiative forcing from anthropogenic aerosols independently of climate feedbacks and atmospheric adjustments. Furthermore, as MACv2-SP provides two distinct prescribed radiative perturbations for the direct and indirect effects of aerosols, we can substitute them one at a time into the PRP method to evaluate their respective contributions. This approach allows us to conduct regular historical simulations in MPI-ESM1.2-CR and investigate the past evolution of anthropogenic aerosol effects on the climate system.

3 Results

In the following section we present the results of the simulated anthropogenic aerosol forcing calculated from our implementation of the PRP. We separate the direct and in-

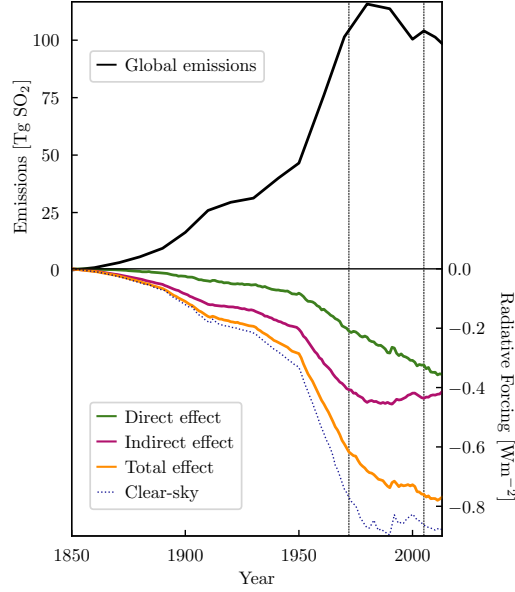


Figure 1. Historical forcing from anthropogenic aerosols. On the top part is shown the historical aerosol emissions and on the bottom part is shown the induced radiative forcing in MPI-ESM1.2-CR. Values are global yearly means. Vertical lines indicate the years 1972 and 2005 when emission levels were similar but led to different total aerosol forcing.

direct effects of aerosols then we present the individual contributions of the different sources of emissions. Finally we investigate the mechanisms governing the regional efficiency of aerosol emissions.

3.1 Historical Aerosol Forcing

Our PRP diagnostic, which assesses anthropogenic aerosol forcing in historical simulations, reveals a consistent and increasing negative forcing from aerosols, despite the global reduction in their emissions (see Fig. 1). This persistent negative trend is primarily driven by the direct effect, which continues to increase even after the implementation of regulations in Europe and North America since the 1980s. Meanwhile, the indirect effect diminishes in approximate proportion to decreasing emissions. In addition to the global decrease in aerosol emissions, the period spanning from 1980 to 2005 witnessed a shift in aerosol patterns. Aerosol concentrations transitioned from being primarily centered in Europe and North America to becoming more concentrated in Southern and Eastern Asian regions. The subsequent sections investigate the role played by this geographical shift in explaining the observed discrepancy between aerosol emissions and the induced forcing.

3.2 Forcing from Regional Aerosol Sources

As detailed in Section 2, MACv2-SP provided a parametrisation for anthropogenic aerosols, incorporating nine distinct simple-plumes that represent various anthropogenic emission regions. To assess the aerosol forcing from each of these regions, we substituted one plume at a time into the PRP (see Sec. 2). Fig. 2 illustrates the resulting forcing values from each region plotted against their respective aerosol emissions (in $[\text{Tg SO}_2]_{eq}$). Regressing the induced forcing against the associated emission level, we obtain a value of the emission efficiency in Wm^{-2} per $[\text{Tg SO}_2]_{eq}$. In Fig. 2.a., we observe a significant

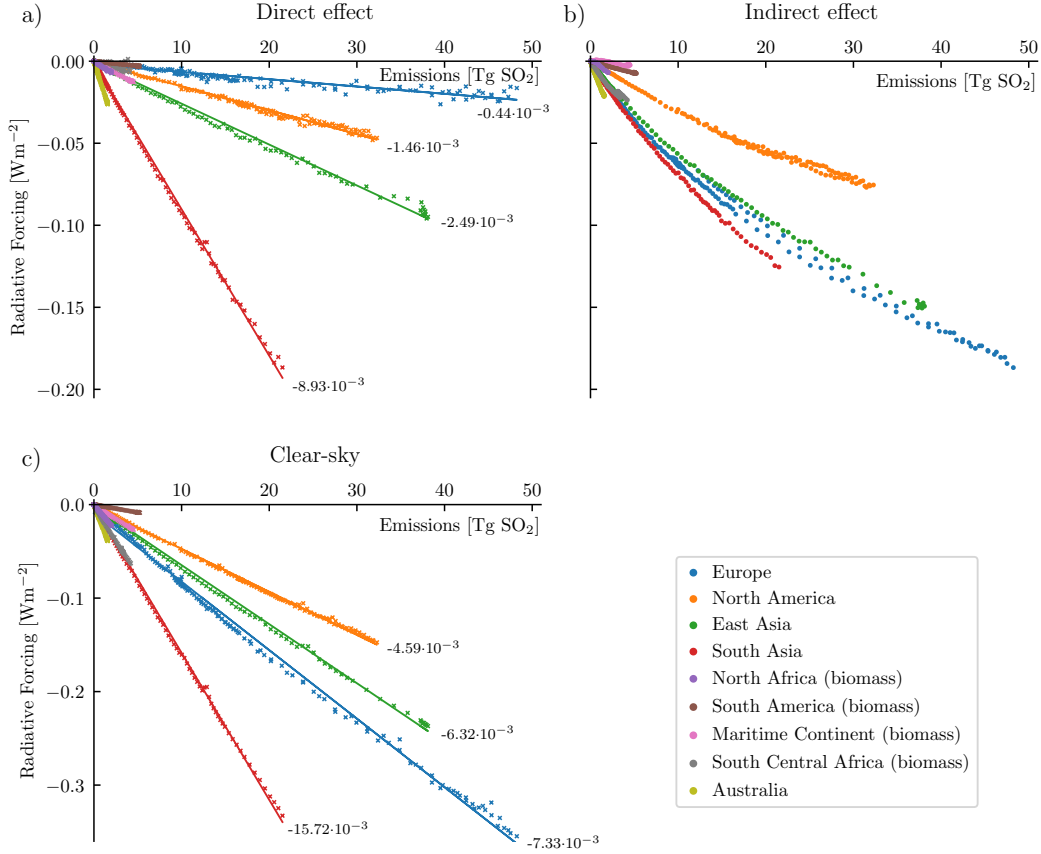


Figure 2. Aerosol forcing from individual emission regions against regional emission levels. Plots are global yearly means with a) is the direct effect, b) is the indirect effect and c) the clear-sky aerosol effect. Values on the plots are the efficiencies in Wm^{-2} per Tg of eqSO_2 of the major emission regions, based on linear regression.

variability in emission efficiency of the direct effect among major industrial regions, such as Europe, North America, East and South Asia, and Australia. Notably, South Asia exhibits an emission efficiency 20.10 times greater than Europe, representing the most substantial difference in efficiency across these regions. On the other hand, Fig. 2.b. shows a relatively more consistent relationship between forcing and emissions for the indirect effect across regions. The regional variation in emission efficiency explains the persistent increase in the global direct effect. Regions with higher efficiencies have a more substantial impact on the global direct effect while emitting fewer aerosols. This effect becomes particularly evident when considering the shift in aerosol patterns from 1980 to 2005. During this period, aerosol emissions shifted from Europe and North America to Southeast Asia, where higher emission efficiencies prevailed. Consequently, despite reduced global emissions during this timeframe, the global aerosol forcing continued to rise. Subsequent sections delve into the mechanisms that underlie these regional variations in aerosol emission efficiency.

3.3 All-sky vs Clear-sky Aerosol Forcing

We examine the outcomes of the PRP performed under both all-sky and clear-sky conditions. The results under all-sky conditions confirm the findings of Huusko et al. (2022):

the direct effect primarily occurs in the vicinity of emission sources (see Fig. 3.c.); in contrast, the indirect effect is more pronounced over remote regions (see Fig. 3.b.) and is larger than the direct effect.

In clear-sky conditions, the global aerosol forcing surpasses the global total forcing (including direct and indirect effects) observed under all-sky conditions (see Fig. 1). It is essential to note that, in clear-sky conditions, only the direct effect applies. Interestingly, the clear-sky aerosol forcing is more than twice as large as the direct effect observed in all-sky conditions. This pattern remains consistent across all emission regions, with clear-sky aerosol forcing consistently exceeding the all-sky direct effect (see Fig. 2.a. and c.). Under all-sky conditions, the presence of extensive cloud cover results in a neutral or positive forcing from the direct effect of aerosols (see Fig. 3.c. and e.). In fact, the presence of clouds moderates the net effect of aerosols while amplifying the net effect of aerosol absorption (Li et al., 2022). Given the values of single-scattering albedo provided by MACv2-SP, which are 0.93 and 0.87 for industrial and biomass burning emissions respectively (Stevens et al., 2017), the positive effect of absorption prevails in the presence of clouds. This results in a net positive direct effect of aerosols. We confirmed this finding with a simulation in which we set the SSA to 1 (indicating no absorption, only scattering), resulting in solely negative direct effect (not shown). This confirms the significant role of aerosol absorption and its influence on the overall forcing in the presence of clouds.

In addition, in regions with persistent cloud systems, the negative forcing arising from the indirect effect through clouds and the positive direct effect tend to balance each other (see Fig. 3.a. and e.). This mechanism has significant implications for regional emission efficiency. In particular, it explains why Europe, which exhibits weak emission efficiency under all-sky (Fig. 2.a.) due to positive direct effect at high latitudes (Fig. 3), demonstrates greater efficiency under clear-sky conditions. Looking at clear-sky conditions significantly narrows the gap in regional efficiencies. In South Asia, the emission efficiency in clear-sky conditions is only 2.1 times greater than in Europe, which is significantly lower than the 20.1 times difference observed in all-sky direct effect. The most pronounced contrast is now seen between South Asia and North America, with South Asia showing an emission efficiency 3.2 times greater than North America.

The interaction between cloud cover and the direct effect of anthropogenic aerosols emerges as a main factor influencing regional emission efficiency. This largely explains the consistent increase in aerosol negative forcing despite reduced emissions. As Southeast Asian regions present less cloud cover at the emission sources compared to Europe, the shift in aerosol patterns results in enhanced global direct effect. The presence of clouds in remote regions, stemming from Southeast Asian emission sources, such as over the Indian and Pacific Oceans, maintains the indirect effect despite the pattern shift. Overall, emission efficiency is greater in Southeast Asian regions compared to Europe and North America. The resulting increase in emission efficiency from the shift in aerosol pattern is critical in the enhanced aerosol forcing observed when comparing the mid-1970s to the mid-2000s, even though emissions levels were similar. However, the disparity in emission efficiencies among regions remains substantial under clear-sky conditions. The following sections investigate the factors contributing to these regional differences.

3.4 Aerosol Removal Processes

The MACv2-SP has been designed to simplify the representation of anthropogenic aerosols in climate models through a straightforward parametrisation. It provides monthly mean Aerosol Optical Depth (AOD) from the ground-based measured 2005 distribution that have been scaled with estimates of historical emissions (Stevens et al., 2017). Consequently, the AOD in MACv2-SP may not always exhibit a direct proportionality to emissions from various regions due to regional variation in aerosol removal processes.

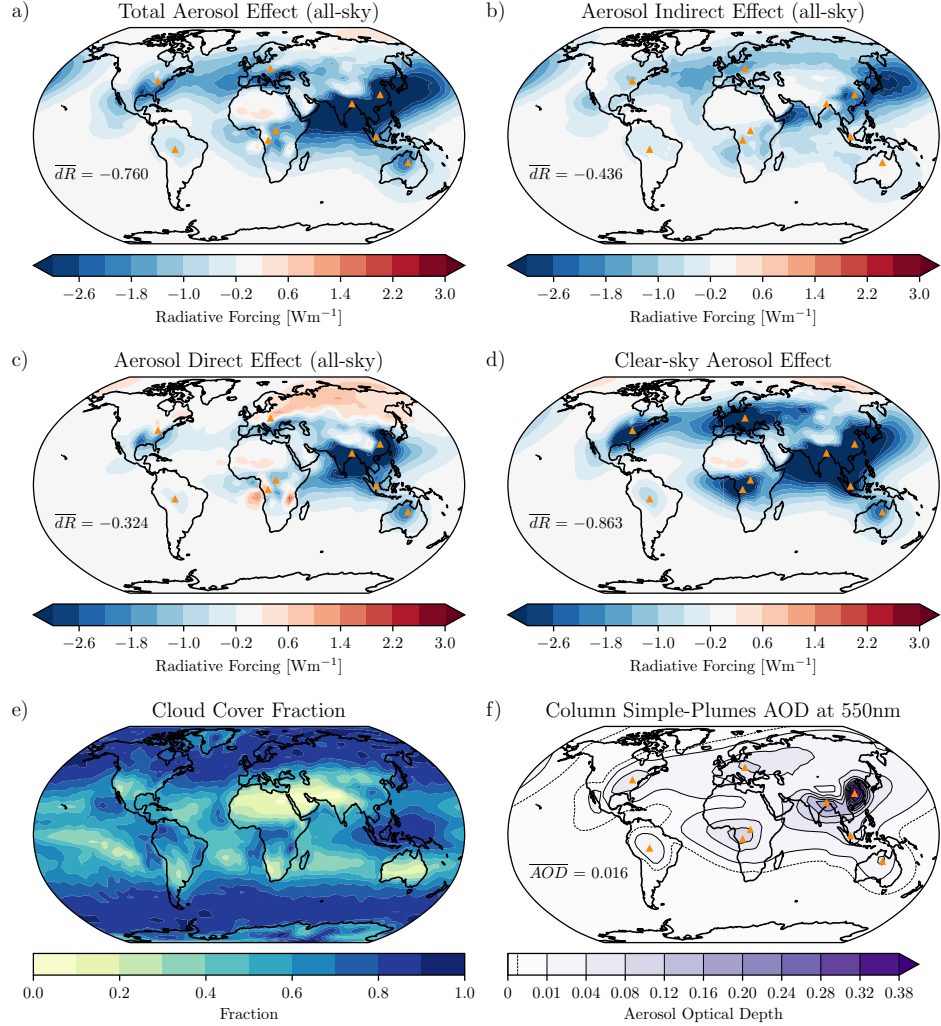


Figure 3. Present-day (2005) aerosol forcing spatial pattern (yearly mean). Shown is a) the total aerosol forcing, separated into b) the indirect effect and c) the direct effect. d) is the clear-sky aerosol effect and e) is the cloud cover fraction. f) the Column Aerosol Optical Depth at 550nm from the MACv2-SP (Simple-Plumes) parametrisation, with dashed-line showing low AOD value contour (0.0025). Values on the maps are global means.

Fig. 4.a. shows the clear-sky aerosol forcing plotted against the corresponding AOD levels for each region. This representation noticeably reduces the difference in emission efficiency between regions. For instance, the efficiency of South Asia is 1.3 greater than that of Europe when measured in Wm^{-2} per unit of AOD, whereas it was 2.1 greater when measured in Wm^{-2} per unit of emissions. Interestingly, when considering AOD levels, both Asian regions exhibit similar efficiencies, which is not the case when considering emissions. This difference arises because storm tracks over the Pacific Ocean play a significant role in aerosol removal. They effectively remove a substantial amount of aerosols, resulting in lower forcing per unit of emissions for East Asia. Conversely, the relatively stable atmospheric conditions over the Indian Ocean contribute to a higher forcing per unit of emissions for South Asia. Similarly, storm tracks over the Atlantic Ocean lead to the efficient removal of aerosols from North America, resulting in a weaker efficiency in forcing relative to emissions. In contrast, aerosols in Europe are transported over longer distances without being removed, leading to a higher efficiency in forcing relative to emissions in clear-sky conditions.

This difference in aerosol removal patterns is the second most important explanation for the continued increase in aerosol forcing despite reduced emissions. The shift in aerosol patterns from Europe and North America towards Southeast Asian regions, with more stable conditions, prolongs the residence time of aerosols in the atmosphere, consequently enhancing the emission efficiency. The last section, we suggest additional explanations for the remaining minor differences in emission efficiency between regions.

3.5 Surface and Aerosol Single-Scattering Albedo

The remaining differences in clear-sky efficiency among industrial regions appear to be closely related to surface albedo (Fig. 4.b.). When multiplied by surface albedo, South Asia efficiency in Wm^{-2} per unit of AOD is only 1.08 greater than Europe (against 1.3 without surface albedo adjustments). Similar to cloud cover in Section 3.3, anthropogenic aerosol forcing also depends on the nature of the underlying surface (Li et al., 2022). In areas with inherently reflective surfaces, aerosol emissions can contribute to the net absorption of shortwave radiation. This clarifies why Europe, which emits aerosols in high-latitudes over snow-covered and icy regions, exhibits weaker efficiency compared to regions with darker surfaces, such as Asia. It's important to note that this effect is primarily observed in clear-sky forcing, as in all-sky conditions, the direct effect is largely influenced by interactions with cloud albedo detailed in Section 3.3. Nonetheless, these findings suggest that a shift in aerosol patterns towards regions with darker surfaces can lead to greater aerosol forcing for similar emission levels.

The distinction between industrial and biomass aerosol emissions affects primarily the Single-Scattering Albedo (SSA) parameter provided by MACv2-SP, which is 0.93 for industrial and 0.87 for biomass (Stevens et al., 2017). This difference explains why the efficiencies of biomass regions remain weaker compared to industrial regions. In Fig. 4.c., we provide an identical representation to Fig. 4.b., but with the SSA of biomass regions set to the same value as for industrial regions, effectively eliminating the disparities. It's important to note that this observation holds true in all-sky conditions as well, as SSA defines the ratio of scattering efficiency to total extinction efficiency. However, it plays a relatively minor role in the overall discrepancy, given that biomass regions typically have smaller emissions and smaller forcing.

4 Discussion and Conclusions

Open Research Section

The source code for MPI-ESM1.2 can be accessed via <https://mpimet.mpg.de/en/science/models/mip-esm> (Mauritsen et al., 2019). Additionally, the specific parts of the code that were mod-

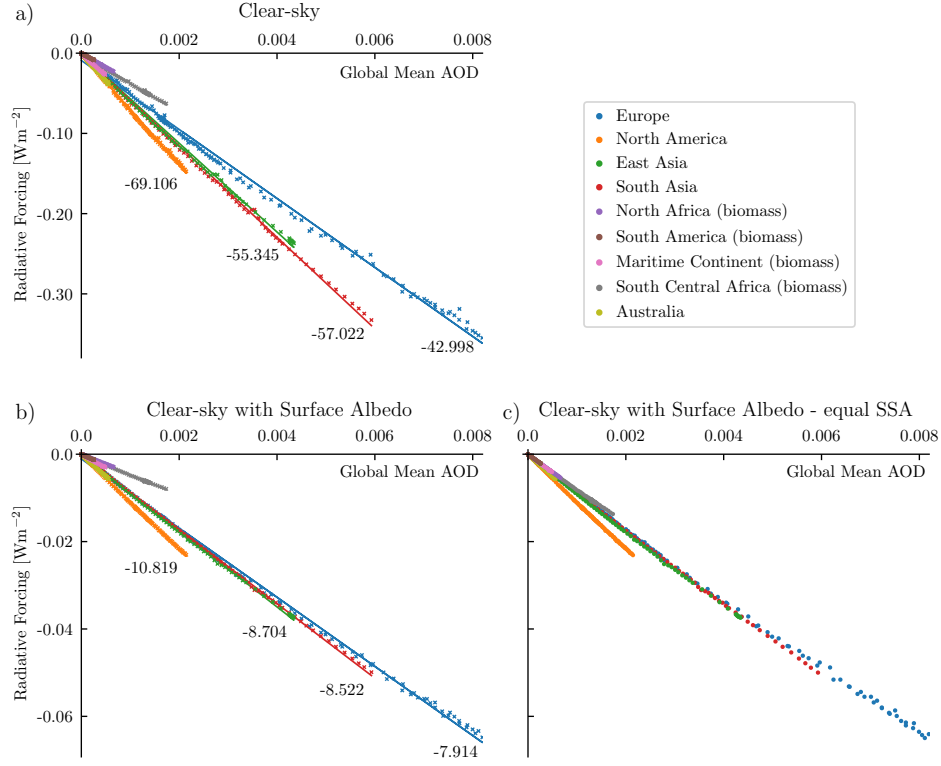


Figure 4. Aerosol forcing from individual emissions regions against regional column aerosol optical depth. Plots are global yearly means with a) showing the clear-sky aerosol effect, b) the clear-sky aerosol effect adjusted by the surface albedo and c) similar to b) but the Single-Scattering Albedo (SSA) was set to the same value for both industrial and biomass burning sources. Values on the plots are the efficiencies in Wm⁻² per unit of AOD of the major emission regions, based on linear regression.

ified or implemented for this study, as well as the output data and Python scripts used in producing the figures presented in this paper, are accessible through Zenodo at
()

Acknowledgments

The computations resources were provided by the National Academic Infrastructure for Supercomputing in Sweden (NAISS) and the Swedish National Infrastructure for Computing (SNIC) at Uppsala Multidisciplinary Center for Advanced Computational Science (UPPMAX) partially funded by the Swedish Research Council through grant agreements no. 2022-06725.

References

- Bellouin, N., Quaas, J., Gryspeerdt, E., Kinne, S., Stier, P., Watson-Parris, D., ... Stevens, B. (2020). Bounding Global Aerosol Radiative Forcing of Climate Change. *Reviews of Geophysics*. Retrieved from <https://agupubs.onlinelibrary.wiley.com/doi/abs/10.1029/2019RG000660> doi: <https://doi.org/10.1029/2019RG000660>
- Block, K., & Mauritsen, T. (2013). Forcing and feedback in the MPI-ESM-LR coupled model under abruptly quadrupled CO₂. *Journal of Advances in Modeling Earth Systems*. doi: 10.1002/jame.20041
- Colman, R. A., & McAvaney, B. J. (1997). A study of general circulation model climate feedbacks determined from perturbed sea surface temperature experiments. *Journal of Geophysical Research: Atmospheres*. doi: 10.1029/97jd00206
- Eyring, V., Bony, S., Meehl, G. A., Senior, C. A., Stevens, B., Stouffer, R. J., & Taylor, K. E. (2016, may). Overview of the coupled model intercomparison project phase 6 (CMIP6) experimental design and organization. *Geoscientific Model Development*, 9(5), 1937–1958. doi: 10.5194/gmd-9-1937-2016
- Fiedler, S., Stevens, B., & Mauritsen, T. (2017, jun). On the sensitivity of anthropogenic aerosol forcing to model-internal variability and parameterizing a Twomey effect. *Journal of Advances in Modeling Earth Systems*, 9(2), 1325–1341. doi: 10.1002/2017ms000932
- Flynn, C. M., Huusko, L., Modak, A., & Mauritsen, T. (2023, jul). Strong aerosol cooling alone does not explain cold-biased mid-century temperatures in CMIP6 models. doi: 10.5194/egusphere-2023-1613
- Flynn, C. M., & Mauritsen, T. (2020). On the climate sensitivity and historical warming evolution in recent coupled model ensembles. *Atmospheric Chemistry and Physics*. doi: 10.5194/acp-20-7829-2020
- Huusko, L., Modak, A., & Mauritsen, T. (2022, oct). Stronger Response to the Aerosol Indirect Effect Due To Cooling in Remote Regions. *Geophysical Research Letters*, 49(21). doi: 10.1029/2022gl101184
- Kinne, S., O'Donnel, D., Stier, P., Kloster, S., Zhang, K., Schmidt, H., ... Stevens, B. (2013, oct). MAC-v1: A new global aerosol climatology for climate studies. *Journal of Advances in Modeling Earth Systems*, 5(4), 704–740. doi: 10.1002/jame.20035
- Klocke, D., Quaas, J., & Stevens, B. (2013). Assessment of different metrics for physical climate feedbacks. *Climate Dynamics*. doi: 10.1007/s00382-013-1757-1
- Li, J., Carlson, B. E., Yung, Y. L., Lv, D., Hansen, J., Penner, J. E., ... Dong, Y. (2022, may). Scattering and absorbing aerosols in the climate system. *Nature Reviews Earth and Environment*, 3(6), 363–379. doi: 10.1038/s43017-022-00296-7

- 305 Mauritsen, T., Bader, J., Becker, T., Behrens, J., Bittner, M., Brokopf, R., ...
 306 Roeckner, E. (2019, apr). Developments in the MPI-M Earth System
 307 Model version 1.2 (MPI-ESM1.2) and Its Response to Increasing CO₂.
 308 *Journal of Advances in Modeling Earth Systems*, 11(4), 998–1038. doi:
 309 10.1029/2018ms001400
- 310 Mauritsen, T., & Roeckner, E. (2020, may). Tuning the MPI-ESM1.2 Global Cli-
 311 mate Model to Improve the Match With Instrumental Record Warming by
 312 Lowering Its Climate Sensitivity. *Journal of Advances in Modeling Earth*
 313 *Systems*, 12(5). doi: 10.1029/2019ms002037
- 314 Meraner, K., Mauritsen, T., & Voigt, A. (2013). Robust increase in equilibrium cli-
 315 mate sensitivity under global warming. *Geophysical Research Letters*. doi: 10
 316 .1002/2013gl058118
- 317 Pincus, R., Forster, P. M., & Stevens, B. (2016, may). The Radiative Forcing Model
 318 Intercomparison Project (RFMIP): Experimental Protocol for CMIP6.
 319 doi: 10.5194/gmd-2016-88
- 320 Stevens, B. (2015, jun). Rethinking the lower bound on aerosol radiative forcing.
 321 *Journal of Climate*, 28(12), 4794–4819. doi: 10.1175/jcli-d-14-00656.1
- 322 Stevens, B., Fiedler, S., Kinne, S., Peters, K., Rast, S., Müsse, J., ... Mauritsen,
 323 T. (2017). MACv2-SP: a parameterization of anthropogenic aerosol optical
 324 properties and an associated Twomey effect for use in CMIP6. *Geoscientific*
 325 *Model Development*. doi: 10.5194/gmd-10-433-2017
- 326 Wetherald, R. T., & Manabe, S. (1988). Cloud Feedback Processes in a General
 327 Circulation Model. *Journal of the Atmospheric Sciences*. doi: 10.1175/1520
 328 -0469(1988)045(1397:cfpiag)2.0.co;2